

1 This submission is intended as an Article, in the Discoveries Section

2 **Title: The neighborhood of the Spike gene is a hotspot for modular intertypic homologous**  
3 **and non-homologous recombination in Coronavirus genomes**

4 Marios Nikolaidis<sup>1</sup>, Panayotis Markoulatos<sup>2</sup>, Yves Van de Peer<sup>3,4,5,6</sup>, Stephen G. Oliver<sup>7</sup>, Grigorios  
5 D. Amoutzias<sup>1</sup>

6 <sup>1</sup>Bioinformatics Laboratory, Department of Biochemistry and Biotechnology, University of  
7 Thessaly, Larissa, 41500, Greece

8 <sup>2</sup>Microbial Biotechnology-Molecular Bacteriology-Virology Laboratory, Department of  
9 Biochemistry and Biotechnology, University of Thessaly, Larissa, 41500, Greece

10 <sup>3</sup>Department of Plant Biotechnology and Bioinformatics, Ghent University, 9054 Ghent, Belgium

11 <sup>4</sup>Center for Plant Systems Biology, VIB, 9054 Ghent, Belgium

12 <sup>5</sup>Department of Biochemistry, Genetics and Microbiology, University of Pretoria, Pretoria 0028,  
13 South Africa

14 <sup>6</sup>College of Horticulture, Nanjing Agricultural University, Nanjing, 210095, China

15 <sup>7</sup>Department of Biochemistry, University of Cambridge, Sanger Building, 80 Tennis Court Road,  
16 Cambridge CB2 1GA, UK

17 To whom correspondence should be addressed. Tel: +30-2410-565289; Fax: +30-2410-565290;

18 Email: [amoutzias@bio.uth.gr](mailto:amoutzias@bio.uth.gr)

19  
20 **Abstract**

21 Coronaviruses (CoVs) have very large RNA viral genomes with a distinct genomic architecture  
22 of core and accessory open reading frames (ORFs). It is of utmost importance to understand their  
23 patterns and limits of homologous and non-homologous recombination, because such events may  
24 affect the emergence of novel CoV strains, alter their host range, infection rate, tissue tropism  
25 pathogenicity, and their ability to escape vaccination programs. Intratypic recombination among  
26 closely related CoVs of the same subgenus has often been reported; however, the patterns and  
27 limits of genomic exchange between more distantly related CoV lineages (intertypic  
28 recombination) needs further investigation. Here, we report computational/evolutionary analyses  
29 that clearly demonstrate a substantial ability for CoVs of different subgenera to recombine.  
30 Furthermore, we show that CoVs can obtain - through non-homologous recombination -  
31 accessory ORFs from core ORFs, exchange accessory ORFs with different CoV genera, with  
32 other viruses (i.e., toroviruses, influenza C/D, reoviruses, rotaviruses, astroviruses) and even with  
33 hosts. Intriguingly, most of these radical events result from double-crossovers surrounding the  
34 Spike ORF, thus highlighting both the instability and mobile nature of this genomic region. While

35 many such events have often occurred during the evolution of various CoVs, the genomic  
36 architecture of the relatively young SARS-CoV/SARS-CoV-2 lineage so far appears to be stable.

37

### 38 **Introduction**

39 Genomic analyses of single-stranded RNA-viruses, including Coronaviruses (CoVs), have  
40 repeatedly demonstrated how recombination affects their emergence, host-range, and  
41 pathogenicity (Decaro et al. 2009; Simon-Loriere and Holmes 2011; Terada et al. 2014; Tian et  
42 al. 2014; Su et al. 2016; Lau et al. 2018). Given the current pandemic of SARS-CoV-2  
43 (Coronaviridae Study Group of the International Committee on Taxonomy of Viruses 2020; Wu  
44 et al. 2020), it is of utmost importance to fully understand the patterns and limits of homologous  
45 and non-homologous genomic exchange of the entire CoV subfamily. This knowledge will allow  
46 us to better evaluate any risks from cross-species transmission and recombination with other  
47 closely or distantly related viruses. It may also guide the development of future vaccines, by  
48 allowing the selection of stable antigenic regions and avoiding reversion (via recombination) of  
49 any future live-attenuated vaccine strains (Guillot et al. 2000; Racaniello 2006; Pliaka et al. 2012;  
50 Burns et al. 2013; Graham et al. 2018; Nikolaidis et al. 2019).

51 According to the ICTV 2020 release, the CoV subfamily (*Orthocoronavirinae*) harbours  
52 significant genomic diversity, comprising 4 genera ( $\alpha$ - $\delta$ ), further subdivided into 25 sub-genera  
53 (Lauber et al. 2012; Lauber and Gorbalenya 2012; ICTV Coronaviridae study group). Various  
54 CoVs are found in a wide range of animal species, causing respiratory, enteric, hepatic, and  
55 nervous system disorders with mild to severe symptoms (Rota et al. 2003; Weiss and Navas-  
56 Martin 2005; Woo et al. 2007; Bermingham et al. 2012; Wheeler et al. 2018; Chen et al. 2020;  
57 Wu et al. 2020). Bats are reservoirs for the  $\alpha$ - and  $\beta$ -CoVs, whereas wild birds are reservoirs for  
58 the  $\gamma$ - and  $\delta$ -CoVs (Woo et al. 2009; Woo et al. 2012; Wong et al. 2019; Latinne et al. 2020;  
59 Wille and Holmes 2020). Human CoVs are found in the  $\alpha$ - and  $\beta$ -genera and have a zoonotic  
60 origin, with bats as the key reservoir, but intermediate hosts may also be involved in the cross-  
61 species transmission (Song et al. 2005; Reusken et al. 2013; Fan et al. 2019).

62 CoVs possess very large genomes among RNA-viruses (25-32 Kb) and contain at least 6  
63 core ORFs (1a, 1b, Spike, Envelope, Membrane, and Nucleocapsid) (Gorbalenya et al. 2006; Cui  
64 et al. 2019; Chen et al. 2020). Lineage-specific accessory ORFs are also present and may be  
65 involved in host adaptation, including the modulation of interferon signaling and the production  
66 of pro-inflammatory cytokines (Gorbalenya et al. 2006; Liu et al. 2014; Cui et al. 2019; Hartenian  
67 et al. 2020). This large genome size and complex architecture allows division of labour and  
68 flexibility for cross-species adaptation (Lauber et al. 2013). Importantly, the Spike protein

69 facilitates binding to host receptors and so determines host-range, cell-tropism, and even the  
70 transition from a mild towards a highly pathogenic phenotype, via point-mutations and  
71 recombination (Sánchez et al. 1999; Kuo et al. 2000; Casais et al. 2003; Rottier et al. 2005;  
72 Menachery et al. 2015).

73         Recombination events among closely-related CoV strains/genotypes/species of the same  
74 subgenus have been reported frequently (Keck et al. 1988; Kottier et al. 1995; Herrewegh et al.  
75 1998; Decaro et al. 2009; Tian et al. 2014; Dudas and Rambaut 2016; Forni et al. 2017; Bobay et  
76 al. 2020; Boni et al. 2020; Saeng-Chuto et al. 2020; Goldstein et al. 2021; Yang et al. 2021); we  
77 denote this category of events as *intratypic* recombination. The corresponding recombination  
78 junctions are scattered across the genome, although enrichment around transcriptional regulatory  
79 sequences (TRS-B) has been reported (Yang et al. 2021). These TRS are needed for template  
80 switching during the transcription of the CoV ORFs (Sawicki et al. 2007; Sola et al. 2015), but  
81 they may also facilitate recombination via template switching among different CoVs (Graham et  
82 al. 2018; Yang et al. 2021). The genomes of several CoVs are mosaic, but many of their donors  
83 have yet to be sequenced (Goldstein et al. 2021). Furthermore, recombination events among more  
84 distantly related CoVs have also been observed. Such radical evolutionary events probably result  
85 from the presence of highly conserved TRS-B sequences (shared between the recombining CoVs)  
86 at the beginning of the various ORFs (Sawicki et al. 2007; Sola et al. 2015; Boniotti et al. 2016;  
87 Graham et al. 2018; Banerjee et al. 2020). Nevertheless, very disparate TRS-B sequences  
88 between two CoVs cause incompatibility and thus may also present barriers to such  
89 recombination events (Yount et al. 2006). In this study, we define as *intertypic* any recombination  
90 event among members of different CoV subgenera. In addition, non-homologous recombination  
91 events may occur with other viruses or taxa, leading to the acquisition of new genomic regions  
92 that appear as lineage-specific accessory ORFs (Zeng et al. 2008; Woo et al. 2014; Forni et al.  
93 2017). The goal of this study is to understand the patterns and limits of radical (intertypic)  
94 genomic exchange of CoVs and to see whether any genomic regions emerge as hotspots of  
95 recombination. The first part of this analysis focuses on homologous recombination of core ORFs  
96 among different CoV subgenera, whereas the second part deals with non-homologous  
97 recombination of accessory ORFs among CoV subgenera/genera and even with other taxa.

98

## 99 **Results**

100

101 Several computational methods exist for detecting and analyzing recombination events among  
102 closely related viruses (Posada et al. 2002; Pond et al. 2005; Martin et al. 2011). In this study, we

103 have implemented phylogenetic tree incongruence methods, which are best suited for macro-  
104 evolutionary analyses, as well as similarity plots (see Methods Sections). BioNJ, PhyML and  
105 Bayesian protein phylogenetic trees and tanglegrams (or ‘cophylo plots’, a way of graphically  
106 representing correspondence between two phylogenies with the same tip labels) were generated  
107 for the non-structural peptides (nsps) of ORFs 1a/1b and the other core ORFs. This was done both  
108 for all four genera together and for each of the four genera individually. In addition, phylogenetic  
109 trees (BioNJ and PhyML) of the various regions were compared against each other for  
110 incongruence, using the normalized Robinson-Foulds method for unrooted trees (see Methods  
111 section). We further validated the statistical significance of detected incongruities with CONSEL,  
112 to ensure the robustness of our conclusions. In this study, we only consider highly confident  
113 phylogenetic incongruence events that are supported by high bootstrap, aLRT and posterior  
114 probability values for all three tree methods and are also statistically supported by the  
115 corresponding CONSEL analyses. In all analyses, the neighborhood of the Spike ORF emerges as  
116 an intertypic recombination hotspot.

117

### 118 **The Spike ORF displays elevated phylogenetic tree incongruence**

119 Phylogenetic trees based on the Spike ORF consistently display the highest or next-highest  
120 phylogenetic incongruence compared to all other analyzed regions, in  $\alpha$ -,  $\gamma$ - and  $\delta$ -CoVs (Figure  
121 1; suppl. file 1 figs 32-33, 38-39, 50-51, 57-58). In contrast, the corresponding regions of  $\beta$ -CoVs  
122 display relatively low phylogenetic incongruence. The Spike sequence is one of the most variable  
123 core genomic regions. However, other core regions also have similar sequence variability, but do  
124 not display such high levels of phylogenetic incongruence. Therefore, this pattern (confirmed by  
125 subsequent phylogenetic tree tanglegram analyses) does not result from badly aligned regions,  
126 rather, it may be attributed to divergence combined with cassette-like intertypic recombination. If  
127 the majority of intertypic recombination events involved single crossovers, then there should be  
128 high phylogenetic incongruence among the regions flanking the Spike ORF, but this is not the  
129 case. Furthermore, if most of the intertypic recombination (in various regions) involved single  
130 crossovers, then the incongruence among the 5’ terminal nsps and the 3’ terminal ORFs, such as  
131 Membrane and Nucleocapsid, should also be high, resembling linkage disequilibrium decay  
132 (Dudas and Rambaut 2016), but it is not.

133

134

135 **Tanglegram-based detection of intertypic recombination events in the common ancestors of**  
136 **CoV genera and subgenera**

137  $\alpha$ - and  $\beta$ -CoVs consistently cluster together as a major clade for all core genomic regions except  
138 for Spike, for which most of the  $\alpha$ - and all the  $\delta$ -CoVs form a single group (Figure 2 and  
139 suppl.fig.1, recombination event 21). Moreover, cryo-electron microscopy has demonstrated that  
140 the Spike proteins of  $\alpha$ - and  $\delta$ -CoVs are structurally more similar to each other (Shang et al.  
141 2018). Thus, at least one recombination event occurred in which the common ancestor of all  $\delta$ -  
142 CoVs obtained a Spike ORF from an  $\alpha$ -CoV ancestor.

143 We also observed several cases of phylogenetic incongruence involving entire subgenera  
144 (mostly in  $\alpha$ -CoVs); they displayed a major shift in their phylogenetic position (for a certain  
145 genomic region), as a monophyletic group. We interpret this as a major event that occurred in the  
146 common ancestor of the representative sequences of that subgenus. Here, we only report cases  
147 well supported by BioNJ, PhyML and Bayesian tree tanglegrams and also statistically supported  
148 (for their incongruence) by CONSEL. The regions that are involved in such events are shown in  
149 Figure 2 and are designated as SgM (Subgenus Movement).

150 More specifically, in  $\alpha$ -CoVs, there exist 14 well-established subgenera, with the  
151 *Ozimops* and *Desmodus* genomes possibly forming two extra subgenera. The first 9 subgenera  
152 (*Decacovirus*, *Pedacovirus*, *Colacovirus*, *Nyctacovirus*, *Minunacovirus*, *Duvinacovirus*,  
153 *Setracovirus*, *Myotacovirus*, *Rhinacovirus*) together with *Ozimops* and *Desmodus* constitute a  
154 major clade that we designate A1. Another two subgenera, (*Tegacovirus*, *Minacovirus*) constitute  
155 a major clade that we designate A2 and is a sister group to A1. *Luchacovirus* (found in rodents),  
156 *Sunacovirus* and *Soracovirus* (both found in shrews) constitute three very diverse additional  
157 clades, that we designate A3, A4 and A5 respectively. The tanglegrams reveal that *Ozimops* is a  
158 sister group to *Decacovirus*, but for nsp16 it pairs with *Minunacovirus* (recombination event 4,  
159 suppl.figs.16-19). The *Rhinacovirus* (A1 clade) nsp8 is no longer part of the A1 clade, but  
160 clusters with the A3 *Luchacovirus* (recombination event 3, suppl.figs.12-15). *Luchacovirus* (A3  
161 clade), moves within the A1 clade for both nsp1 (recombination event 1, suppl.figs.4-7) and nsp7  
162 (recombination event 2, suppl.figs.8-11). Similarly, *Sunacovirus* (A4 clade) moves within the A1  
163 clade for Envelope (recombination event 11, suppl.figs.28-31). We observed many other  
164 incongruities for most of the subgenera in various genomic regions, but their new positions (in the  
165 trees) were not supported by both high bootstrap/aLRT values and different trees, thus they may  
166 actually represent cases of rapid divergence.

167           Although  $\alpha$ -CoVs form 5 distinct lineages, their Spike ORFs are organized into two  
168 major evolutionary clusters. The smaller cluster comprises *Rhinacovirus* (a member of clade A1),  
169 *Luchacovirus* (clade A3), *Sunacovirus* (clade A4), *Soracovirus* (clade A5), whereas the major  
170 cluster comprises all the other members of clades A1 and A2 (see Spike tree in Figure 2,  
171 recombination events 5, 8, 9, 10 in suppl.figs.1-2, 20-23,). The Spike ORF of this smaller cluster  
172 has been suggested to originate from  $\beta$ -CoVs via an ancient recombination event (Tsoleridis et al.  
173 2019).

174           Phylogenetic incongruence was also observed for the Nucleocapsid region of  $\beta$ -CoV  
175 *Merbecovirus* (Figure 2 and recombination event 12 in suppl.figs.34-37). By taking *Sarbecovirus*  
176 as the reference point, *Hibecovirus* is their closest subgenus, followed by *Nobecovirus*,  
177 *Merbecovirus*, and finally *Embecovirus* (most distant). The only exception to this pattern is  
178 observed in the Nucleocapsid region, where *Merbecovirus* seems to be the closest subgenus to the  
179 *Sarbecovirus-Hibecovirus* group. An alternative explanation is that the ancestral *Nobecovirus*  
180 Nucleocapsids underwent recombination or significant sequence divergence. However, manual  
181 inspection of the trees, their branch lengths, and the Poisson-distances leads us to favor the first  
182 explanation, whilst acknowledging that the second cannot be excluded at present.

183

#### 184 **Tanglegram-based detection of intertypic recombination between some members of** 185 **different subgenera**

186 We investigated instances where certain genomic regions of the members of a particular subgenus  
187 did not form a monophyletic group. These observations could be attributed to rapid divergence or  
188 intertypic recombination events in some, but not all, members. These events are more recent than  
189 the ones (described above) that occurred in the common ancestor of a subgenus. Such regions are  
190 shown in Figure 2 (designated as “P”: polyphyletic). We checked whether these candidate  
191 recombinant sequences clustered within or next to other subgenera with high  
192 bootstrap/aLRT/posterior probability values and also performed similarity plot and bootscan  
193 analyses with RDP4 (Martin et al. 2015) (see Methods), whenever possible. We detected several  
194 events; two in  $\alpha$ -CoVs, five in  $\gamma$ -CoVs, and three in  $\delta$ -CoVs. Interestingly, 9 of these 10 events  
195 are located at the Spike ORF.

196           The most striking and recent event has been documented for Swine Enteric CoV  
197 (Boniotti et al. 2016), which is essentially a swine *Tegacovirus* (A2 lineage) that obtained the  
198 Spike ORF of a swine *Pedacovirus* (A1 lineage) (recombination event 6, suppl.figs.20-22, 24-  
199 25). A second case (again in the Spike ORF) concerns five of the thirteen analyzed *Tegacovirus*  
200 sequences that form a monophyletic sister group to *Minacoviruses* (recombination event 7,

201 suppl.figs.20-22, 26-27). An alternative sequence of events is that the other seven *Tegacovirus*  
202 (from cats and dogs) that form the second Spike monophyletic group recombined with an as yet  
203 unknown donor from the A2 lineage. Inspection of the phylogenetic trees and their branches leads  
204 us to favor the first option, while the host-range of the second group favors the second option. Yet  
205 another instance concerns four  $\gamma$ -CoV *Igacovirus* Spike sequences (from birds) that form a  
206 monophyletic cluster outside of the *Igacovirus* (recombination events 13-16, suppl.figs.40-44).  
207 This is a case of three or most probably four independent events where members from an as yet  
208 unknown  $\gamma$ -CoV subgenus repeatedly served as Spike donors to several *Igacoviruses*. A further  
209 case involves a duck *Igacovirus* Membrane sequence that clusters with the  $\gamma$ -CoV *Brangacovirus*  
210 (recombination event 17, suppl.figs.45-49). A final example concerns five  $\delta$ -CoV *Buldecovirus*  
211 Spike sequences forming a monophyletic cluster (that is outside of *Buldecoviruses*) and is a sister  
212 group to *Herdecovirus* (recombination events 18-20, suppl.figs.52-56). Our interpretation is that  
213 this is a case of three independent events, where members from an, as yet unknown,  $\delta$ -CoV  
214 subgenus (a close relative of *Herdecoviruses*) repeatedly served as Spike donors to these  
215 *Buldecoviruses*.

216 In addition, we detected several low-confidence intertypic recombination events for  $\alpha$ -  
217 CoV subgenera, where the incongruent sequences cluster with other subgenera, but with low  
218 bootstrap/aLRT/posterior probability support. Here, either the donor is unknown or the  
219 incongruence is due to rapid divergence; they were not considered further in our study. Finally,  
220 we also observed previously reported intratypic recombination events, i.e. within *Sarbecovirus*  
221 (Suppl.Figs.60-68). Although such events are not the focus of this study, it should be mentioned  
222 that, at the beginning of the COVID-19 pandemic, several studies analyzed the available genomic  
223 data for evidence of recombination that could have led to the emergence of SARS-CoV2 (Boni et  
224 al. 2020; Lam et al. 2020; Paraskevis et al. 2020; Yang et al. 2021). Although the data show that  
225 SARS-CoV2 did not emerge via a recent recombination event, recombinant sequences (from  
226 other species) among the SARS-CoV and SARS-CoV2 lineages have been detected and were also  
227 confirmed by our study.

228

229 **Accessory ORF evolution: Non-homologous recombination of accessory ORFs between**  
230 **different CoV subgenera and genera.**

231 Based on PSI-BLAST, we built position-specific scoring matrices (PSSMs) for the various  
232 annotated accessory ORFs and thus identified 73 non-redundant Accessory ORF Families (AOFs;  
233 see Methods Section). The PSSMs allowed for a very sensitive homology search and revealed  
234 very distinct distributions in the various genera and subgenera (Figure 3, Figure 4 and suppl.file

235 2). Although no AOF was present in all four genera, three AOFs were present in some subgenera  
236 of both  $\alpha$ - and  $\beta$ -CoVs and three AOFs were present in subgenera of both  $\gamma$ - and  $\delta$ -CoVs.  
237 Interestingly, three of these intergenus AOFs are localized in the neighborhood of the Spike ORF.  
238 Possibly, some AOFs with restricted distributions may actually be distant homologs of other  
239 AOFs that significantly diverged (Ouzounis 2020; Neches et al. 2021) and lost their homology  
240 signal.

241 Intriguingly, we detected two AOFs with very restricted distributions that originated  
242 either from gene duplication or horizontal gene transfer (HGT) of a Spike ORF fragment. The  
243 first instance concerns a bat  $\beta$ -CoV *Hibecovirus* ORF2 that is situated between ORF1ab and  
244 Spike, that is distantly homologous to the N-terminal region of its Spike (suppl.file 2:  
245 PSSM\_TBlastN: 4e-39; 27% identity). This is either a case of non-homologous  
246 recombination/gene-fragment duplication within the same genome (followed by rapid  
247 divergence) or horizontal transfer from another related *Hibecovirus* Spike N-terminal region. The  
248 second instance concerns a similar Spike gene-fragment duplication event for ORF6 of some  
249 Luchacoviruses (suppl.file 2: PSSM\_TBlastN: 7e-63; 25% identity).

250 We also detected distant homology between the ORF3a of  $\beta$ -CoV  
251 *Sarbecovirus/Hibecovirus/Nobecovirus* and the Membrane ORF of  $\alpha$ -CoV A2 *Tegacovirus* and  
252 A4 *Sunacovirus* (suppl.file 2: PSSM\_TBlastN: 2.4e-4 and 3.9e-4 respectively). Accordingly, a  
253 bioinformatics analysis (Ouzounis, 2020) recently reported a very distant homology among the  
254 SARS-CoV-2 ORF3a and Membrane ORFs. Based on our extended genome sampling and the  
255 observed e-values of the ORF3a PSSM against  $\alpha$ -CoVs (best PSSM\_TBlastN: 2.4e-4) and  $\beta$ -  
256 CoVs (best PSSM\_TBlastN: 2e-3), possibly a Membrane region from  $\alpha$ -CoVs jumped via non-  
257 homologous recombination to the common ancestor of *Sarbecovirus/Hibecovirus/Nobecovirus*  
258 and rapidly diverged to an accessory ORF.

259

#### 260 **Non-homologous recombination of accessory ORFs between coronaviruses and other taxa**

261 We detected seven AOFs that had homologs in other taxa, outside of the *Coronavirinae*  
262 (suppl.file 2), with three of them situated in the neighborhood of Spike. The most striking and  
263 well-studied example is a hemagglutinin-esterase (MHV\_HE) that is present in all the members  
264 of  $\beta$ -CoV *Embecovirus*, situated just before the Spike. It has homologs in toroviruses (porcine  
265 torovirus PSI-Blast e-value: 1.7e-55) and influenza C/D. Most probably, it was acquired either  
266 indirectly (via a torovirus intermediate step) or directly from an influenza C/D-like virus, and  
267 subsequently adapted and coevolved with the Spike (Snijder et al. 1991; Zeng et al. 2008; Caprari  
268 et al. 2015; Lang et al. 2020).



269 Another case is the  $\beta$ -CoV NS2 *Embecovirus* AOF (MHV\_NS2), that belongs to the 2H  
270 phosphoesterase superfamily (Mazumder et al. 2002). This AOF is observed in most  
271 *Embecoviruses*, like HCoV-OC43, and is situated between ORF1ab and the hemagglutinin-  
272 esterase (HE). Interestingly, close homologs (NCBI-BlastP e-value: 6e-61) of this AOF (from  $\beta$ -  
273 CoVs) are consistently found in several rodent  $\alpha$ -CoV *Luchacoviruses* as well (Tsoleridis et al.  
274 2019), at the same genomic location, but they do not have the neighboring HE ORF. This AOF is  
275 also homologous to a region within the central part of polyprotein 1ab of several toroviruses,  
276 including porcine torovirus (PSI-BLAST e-value: 2e-28). Apparently, non-homologous genomic  
277 exchange among CoVs and toroviruses has happened more than once.

278 Next to the  $\alpha$ -CoV *Luchacovirus* ORF2/NS2, there exists another accessory ORF  
279 (instead of HE in *Embecoviruses*), designated ORF2b. It is present in some, but not all  $\alpha$ -CoV  
280 *Luchacoviruses*. It is homologous to rodent C-type lectins (PSI-Blast e-value: 4e-34) found in  
281 natural killer cell receptors as well as in many poxviruses and some herpesviruses. This AOF  
282 probably originated from its hosts (Wang et al. 2020). Furthermore, both ORF2a and ORF2b are  
283 missing from another closely related *Luchacovirus* genome (MT820625.1), thus highlighting the  
284 dynamic nature of this genomic region (Wang et al. 2020) and the potential for gene loss (Forni et  
285 al. 2017).

286 We also identified four more interesting AOFs. p10, situated just after the nucleocapsid  
287 region of some  $\beta$ -CoV *Nobecoviruses* in bats, is homologous (PSI-BLAST e-value: 3.9e-22) to  
288 p10 proteins from reoviruses (Huang et al. 2016). The *Buldecovirus* NS7a AOF (situated after the  
289 Nucleocapsid) of several avian  $\delta$ -CoV *Buldecoviruses* is homologous (PSI-BLAST e-value: 1e-  
290 10) to NSP1-1 from avian rotavirus-g. An uridine kinase (closest PSI-Blast hit: fungi; e-value: 2e-  
291 30) is found only in  $\gamma$ -CoV *Cegacoviruses* (Mihindukulasuriya et al. 2008). Finally, the same  $\gamma$ -  
292 CoV *Cegacoviruses* contain ORF6 that is distantly homologous to the capsid protein of human  
293 astrovirus 5 (PSI-BLAST e-value: 4.7e-7).

294

## 295 **Discussion**

296 The integration of our extensive phylogenetic and genome architecture analyses have revealed  
297 intertypic homologous and non-homologous recombination events among the genomes of  
298 different CoV subgenera/genera, and even with other taxa. Intriguingly, many of these events are  
299 localized around the Spike ORF and occur as double crossovers, where an entire region is  
300 exchanged as a cassette/module and the rest of the genome stays intact. It is unlikely that these  
301 observed and statistically supported phylogenetic incongruities (especially for Spike) are artifacts

302 of rapid divergence or convergent evolution, because the “incongruent” regions actually cluster  
303 with regions from other genera/subgenera with high bootstrap/aLRT/posterior probability support  
304 (among other evidence, like site-wise likelihood of alternative hypotheses – results not shown).  
305 The Spike recombination of Swine Enteric CoV is the most recent and clear example. We have  
306 applied stringent analysis criteria involving the phylogeny of entire regions and it is possible that  
307 many genuine intertypic recombination events may not have passed our filters, especially if they  
308 involved small segments of an ORF (Forni et al. 2017). Another major problem is genomic  
309 sampling, where the donor has yet to be sequenced (Goldstein et al. 2021).

310 Our interpretation for the frequently observed modular recombination events around the  
311 Spike ORF is that long-range genetic interactions of various genomic regions may actually block  
312 radical (intertypic) single crossover recombination events (Sola et al. 2011; Sola et al. 2015) but  
313 allow for double crossover events in certain genomic islands. This conclusion is supported by  
314 various independent experimental observations. Nucleocapsid proteins (N-proteins) from  
315 different members of the same genus may only be partially compatible, whereas N-proteins from  
316 different genera are completely incompatible (Schelle et al. 2005; Sungsuwan et al. 2020) and  
317 may even have a suppressive effect (Masters 2019; Sungsuwan et al. 2020). N-proteins are also  
318 involved in circularization of the genome (Lo et al. 2019). CoV RNA secondary structures have  
319 been shown to form long-range interactions within a CoV genome (Ziv et al. 2020) and to interact  
320 with cellular components, to initiate transcription and replication (Sola et al. 2011). Genetic  
321 interactions have been observed between the nsp8, nsp9 peptides (from ORF1a) and the  
322 pseudoknot at the 3’ end of the genome (Züst et al. 2008). Thus, single-crossover recombination  
323 events among different subgenera may break such long-range interactions, while double-  
324 crossover/modular events may allow their retention.

325 We also observed distinct subgenus-specific accessory ORF genomic architectures. These  
326 may function as an additional barrier to single-crossover intertypic recombination events, that  
327 would otherwise disrupt certain co-evolved combinations of ORFs. Several of these AOFs have  
328 been introduced from other genera/subgenera. However, some of these AOFs do not have  
329 homologs in any other subgenera and may have emerged via i) *de novo* gene birth, ii) rapid  
330 divergence of existing ORFs and loss of the homology signal, or iii) via non-homologous  
331 recombination with ORFs (followed by rapid divergence) from other CoVs, other viruses, or even  
332 hosts (Elhaik et al. 2006; McLysaght and Hurst 2016; Moyers and Zhang 2016; Schmitz and  
333 Bornberg-Bauer 2017; Ouzounis 2020).

334 We observed exchange of genomic regions between CoVs and toroviruses, influenza C/D  
335 (directly or indirectly), reoviruses, rotaviruses, astroviruses, and even with hosts. Such events

336 were frequent in the neighborhood of the Spike ORF. Toroviruses are of particular interest,  
337 because they belong to the same order (*Nidovirales*) as CoVs and can also act as gene donors in  
338 other viral orders, e.g. porcine *Enterovirus-G* (Shang et al. 2017; Hu et al. 2019). Worryingly,  
339 porcine toroviruses have both a worldwide distribution and a high infection rate (Hu et al. 2019).  
340 Thus, future genomic sampling of yet undiscovered CoVs may reveal an even more extensive  
341 exchange between CoVs and toroviruses. Moreover, genomic exchange between viruses  
342 (*Flaviviridae*, *Hepeviridae*, *Dicistroviridae*, *Potyviridae*) and their hosts has been observed  
343 repeatedly (Gilbert and Cordaux 2017). It is conceivable that some of the above-mentioned CoV  
344 AOFs did not move from one virus to the other, but independently from similar hosts; however,  
345 the PSI-Blast results show other viral sequences, and not cellular proteins, to be the closest hits.

346         Importantly, members of the relatively young (Boni et al. 2020) SARS-CoV/SARS-CoV-  
347 2 lineages (within Sarbecoviruses) do not yet appear to act as recipients in radical intertypic  
348 recombination events. They also display a very distinct AOF architecture. Thus, current  
349 evolutionary data do not favor a scenario where SARS-CoV-2 may (homologously) recombine  
350 with other currently circulating human CoVs of other subgenera/genera. Furthermore, SARS-  
351 CoV/SARS-CoV-2 do not seem to exchange accessory ORFs with other CoV subgenera or other  
352 viruses/hosts, with the exceptions of ORF3a that is an old and unresolved event and ORF7a (with  
353 some Decacoviruses). It should be noted that their closest relatives, Hibeoviruses, have a  
354 divergent Spike-like accessory ORF that resulted from either a gene duplication or horizontal  
355 transfer event. Nevertheless, SARS-like viruses can recombine with SARS2-like viruses, as our  
356 and other analyses have shown (Boni et al. 2020; Lam et al. 2020; Yang et al. 2021). This finding  
357 has very important implications, because, combined with the ability of Sarbecoviruses to easily  
358 move from one host to another, it demonstrates a potential for a future intratypic recombination  
359 event (within Sarbecoviruses), where a highly infectious SARS-CoV2 variant (e.g. the Delta  
360 variant) could recombine with a SARS-like sequence in another host species and give rise to a  
361 recombinant that combines the high infectivity of SARS-CoV2 with the much higher mortality  
362 rate of SARS itself.

363         Many of the events that we have observed are very old; nevertheless, our results suggest  
364 that researchers and those responsible for public health should be vigilant. Certain key taxa like  
365 bats and/or farmed animals (especially pigs) have the potential to play a key role in any future  
366 emergence of a recombinant SARS-CoV-2 strain or some other CoV epidemic (from another  
367 genus/subgenus). SARS-CoV-2 spill-back from humans to other animals (domesticated or wild)  
368 that also harbor many and diverse CoVs has been reported (de Moraes et al. 2020; Olival et al.  
369 2020; Sit et al. 2020). Ferrets, cats and dogs are susceptible to the currently circulating SARS-

370 CoV-2 strains, whereas pigs, chicken and ducks appear to have lesser, or no susceptibility  
371 (Meekins et al. 2020; Shi et al. 2020; Sit et al. 2020; Pickering et al. 2021). CoVs demonstrate a  
372 high capacity for cross-species infection, even from birds to mammals, either directly or via a few  
373 evolutionary steps (Li et al. 2006; Graham and Baric 2010; Menachery et al. 2015; Menachery et  
374 al. 2016; Li et al. 2018; Boley et al. 2020). Furthermore, pigs are carriers of very diverse  $\alpha$ -,  $\beta$ -,  
375 as well as  $\delta$ -CoVs and have been shown to function as “recombination bioreactors”, with the  
376 notable example of Swine Enteric CoV (Boniotti et al. 2016). In addition, intensively farmed pigs  
377 are hosts for many other viruses, such as toroviruses or influenza A (Hu et al. 2019; Henritzi et al.  
378 2020; Sun et al. 2020). Fortunately, genomics is a valuable new tool for monitoring the  
379 emergence, spread, and ongoing adaptations of SARS-CoV-2 (Boni et al. 2020; Neches et al.  
380 2020; Worobey et al. 2020; Kemp et al. 2021; Volz et al. 2021). It is conceivable that what we  
381 have observed is only the “tip of the iceberg”; that past unknown recombination events of various  
382 CoVs may have led to many unnoticed (or, perhaps, readily contained) localized small-scale  
383 epidemics that died out. However, given the observed genomic diversity and inherent genomic  
384 instability of CoVs, in this new era of urbanization, global transport, intensive farming, and  
385 habitat destruction (Beyer et al. 2021), intratypic and intertypic recombination events may lead to  
386 new epidemic strains that may prove much more difficult to contain (Bedford et al. 2019). As a  
387 final note, these results highlight the need to further investigate the inclusion of other, and much  
388 more stable, genomic regions (in addition to Spike) in the design and development of the next  
389 generation of coronavirus vaccines.

390

## 391 **Methods**

### 392 **Phylogenetic analyses**

393 We obtained the taxonomy IDs for  $\alpha$ -,  $\beta$ -,  $\gamma$ - and  $\delta$ -CoVs from NCBI Taxonomy in order to  
394 search for available nucleotide sequences in Genbank (Benson et al. 2013), using (as two extra  
395 criteria) the keyword “complete” and nucleotide length higher than 24,000. We obtained 1102,  
396 14769, 435 and 154 genomic sequences from  $\alpha$ -,  $\beta$ -,  $\gamma$ - and  $\delta$ -CoVs respectively, in August 2020.  
397 Redundancy with the set of retrieved sequences was removed with the UCLUST software (Edgar  
398 2010), using 90% nucleotide identity and 98% query coverage at the whole-genome level, in  
399 order to filter out the thousands of available genomes from the same virus that have been  
400 involved in large outbreaks, like SARS-CoV-2, PEDV, IBV. From each non-redundant group, we  
401 retained one representative sequence, or more if they were obtained from different hosts. We  
402 designate these groups as NRG90 (Non-Redundant-Group-90% nucleotide sequence identity). In  
403 addition, within each NRG90 group we ensured that we retained the representative RefSeq

404 sequences for each species, that were obtained from ICTV taxonomy (ICTV Coronaviridae study  
405 group). Sequences were aligned with Muscle (Edgar 2004) and MAFFT (parameters: --auto)  
406 (Nakamura et al. 2018). Multiple alignment views and manual editing were performed with the  
407 Seaview4 software (Gouy et al. 2010). The boundaries of nsps within ORF1ab, as well as those of  
408 Spike, Envelope, Membrane, Nucleocapsid and the accessory ORFs were determined based on  
409 Genbank annotation and from manual inspection of the multiple alignments. Filtering of poorly  
410 aligned regions was performed with the g-blocks software (Castresana 2000), where we retained  
411 sites with less than 50% gaps and blocks of two consecutive sites. Model selection for ML and  
412 Bayesian trees was performed with Prottest3 (Darriba et al. 2011). Subsequent ML tree  
413 reconstruction was performed with PhyML (Guindon and Gascuel 2003) (applying SH-like  
414 approximate likelihood ratio test, SPR algorithm for tree search). Neighbour-Joining (BioNJ)  
415 trees were generated with Seaview4 (Gouy et al. 2010), using the Kimura two-parameter and  
416 Poisson models with 500 bootstraps, for nucleotide and protein sequences, respectively. Bayesian  
417 phylogenetic trees were calculated using the BEAST software v.1.10.4 (Drummond et al. 2012;  
418 Suchard et al. 2018) with MCMC length of 1 million and a burn-in value of 10000 (all the other  
419 operators and priors were set to default). Phylogenetic trees were visualized with Treedyn  
420 (Chevenet et al. 2006), iTOL (Letunic and Bork 2019) and Dendroscope (Huson and Scornavacca  
421 2012). Phylogenetic trees were generated for all regions (nsps, ORF1ab, Spike, Envelope,  
422 Membrane, Nucleocapsid) of each CoV genus independently. In addition, phylogenetic trees that  
423 included all sequences of all four CoV genera together were generated for those regions (nsps 3-  
424 10, 12-16, ORF1ab, Spike, Membrane, Nucleocapsid) whose multiple alignments had a sufficient  
425 number of columns, after g-blocks filtering.

426 Phylogenetic tree incongruence was estimated/quantified with the Robinson-Foulds (RF)  
427 method (Robinson and Foulds 1981) for unrooted trees, within the Visual Treecmp server  
428 (Goluch et al. 2020). A certain genomic region is considered incongruent when its phylogeny is  
429 not in agreement with the phylogeny of the other regions (from the same genome). Visualization  
430 of the triangular matrix of Robinson-Foulds normalized values among the various trees was  
431 performed with Python and R heatmap packages. This RF-matrix resembles the Linkage-  
432 Disequilibrium matrix, at the macroevolutionary level, but for specified genomic regions. Since  
433 the goal was to investigate incongruence at the macroevolutionary level and not within the virus  
434 species level, for this type of analyses, branches with length less than 0.02 were collapsed with  
435 the TreeGraph v2 software (Stöver and Müller 2010). Otherwise, the incongruence of strains of  
436 the same virus species would artificially inflate the RF values. This would especially be the case  
437 for  $\gamma$ -CoVs, where many divergent strains of IBV (*Igacovirus*) were available. Phylogenetic tree

438 tanglegrams were visualized with Dendroscope (Huson and Scornavacca 2012), using the ML,  
439 BioNJ and Bayesian tree of ORF1ab as the reference tree against each of the ML, BioNJ and  
440 Bayesian trees of the individual nsps and ORFs S, E, M, N, for each of the four CoV genera  
441 separately. Estimation of evolutionary distance among homologous aligned sequence regions (for  
442 visualization in the RF-matrices) was performed with the Poisson-distance method within the  
443 MEGA X software (Kumar et al. 2018) (parameters - gap missing data: pairwise deletion; rates  
444 among sites: uniform). The statistical significance of phylogenetic incongruence of specific  
445 suspected recombination events was further assessed with the approximately unbiased (AU) test,  
446 using CONSEL (Shimodaira and Hasegawa 2001). For a certain set of sequences, the reference  
447 PhyML tree was obtained from the suspected recombined region and it was compared against the  
448 PhyML tree of the corresponding ORF1ab regions.

449

#### 450 **Accessory ORF analysis**

451 In the first step of this analysis, all annotated accessory ORFs from our non-redundant set of 196  
452 CoV genomes were retrieved from Genbank. We only retained accessory ORFs with a length  $\geq 50$   
453 amino acids, with the exception of human CoVs (length  $\geq 30$ ) that were situated in the regions  
454 among the 6 core ORFs and not any accessory ORFs that were entirely overlapping with any of  
455 the core ORFs. The selected annotated accessory ORFs in all analyzed genomes were further  
456 clustered in 88 homologous groups, using as cut-off, pairwise BLASTP e-values of  $1e-10$ ,  
457 followed by grouping with mcl-clustering (Enright et al. 2002). Afterwards, a representative  
458 peptide sequence from each cluster was used to build a corresponding Position Specific Scoring  
459 Matrix (PSSM) with locally installed PSI-BLAST, against the *Coronaviridae* proteins of the  
460 (locally installed) NCBI non-redundant protein database, with an e-value cut-off  $1e-3$  and as  
461 many iterations as needed, until convergence was achieved. Next, 15 redundant PSSMs were  
462 removed and we ended up with 73 annotated accessory ORF PSSMs. Accordingly, each non-  
463 redundant PSSM corresponded to one homologous Accessory ORF Family (AOF). All 73  
464 PSSMs are available in supplementary file 3.

465         Afterwards, each AOF PSSM was used to scan all the analyzed CoV representative  
466 genomes for the presence of the corresponding family with TBlastN (cutoff:  $1e-3$ ). Each TBlastN  
467 hit was inspected to determine whether it encoded a peptide of at least 30 amino acids, otherwise  
468 it was considered to be pseudogenized (represented with orange colour in the matrices of figures  
469 3 and 4). The coordinates of the detected homologous regions were visualized in each genome  
470 with Biopython and the genomic architectures were manually inspected. Genomic regions from  
471 the representative CoV genomes containing a certain AOF were aligned with Muscle. Each

472 multiple alignment is available within the zipped supplementary file 4. Next, the annotated ORF  
 473 PSSMs were used as queries to scan the entire NCBI non-redundant protein database, in order to  
 474 detect AOF homologs in taxa outside of *Coronavirinae* and thus detect potential non-homologous  
 475 recombination events (horizontal gene transfers). Intriguingly, bacterial draft genomes were  
 476 found to include CoV AOFs with very high sequence identity. These draft genomes were re-  
 477 assembled with Spades (Bankevich et al. 2012) and the relevant contigs were manually  
 478 investigated for co-presence of CoV and bacterial genes, but they eventually appeared to be  
 479 contaminations and were not further investigated.

480

481 **Figures**

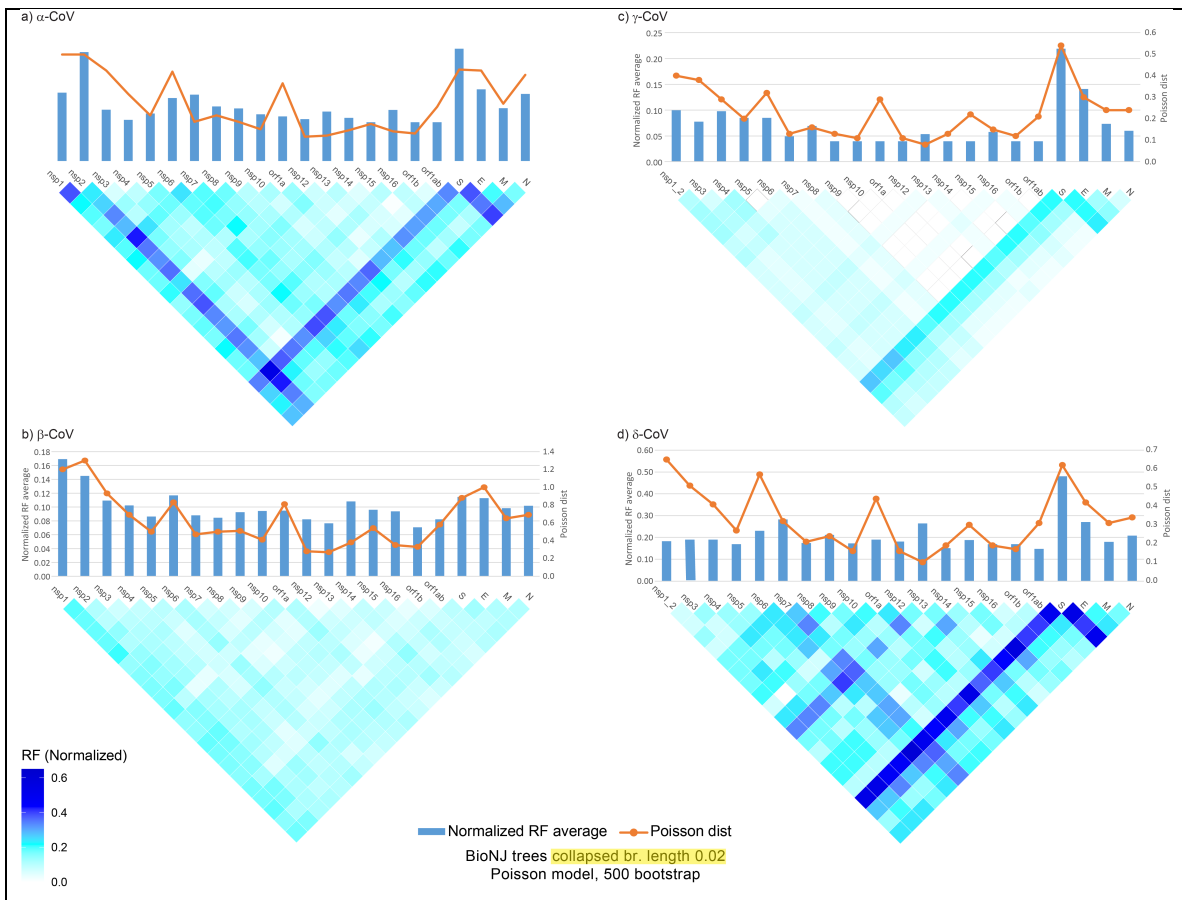


Figure 1. Matrices of incongruence among the core genomic regions of the four CoV genera based on the normalized Robinson-Foulds method, for unrooted trees (calculated with the TreeCMP server). BioNJ phylogenetic trees were generated with the Poisson model of evolution and 500 bootstrap replicates. In addition, branch lengths < 0.02 were collapsed. The orange line above each matrix displays the average Poisson-distance among sequences of the same genomic

region (calculated with the MegaX software). Blue bars above each matrix display the average RF value for that particular region (against all other regions).



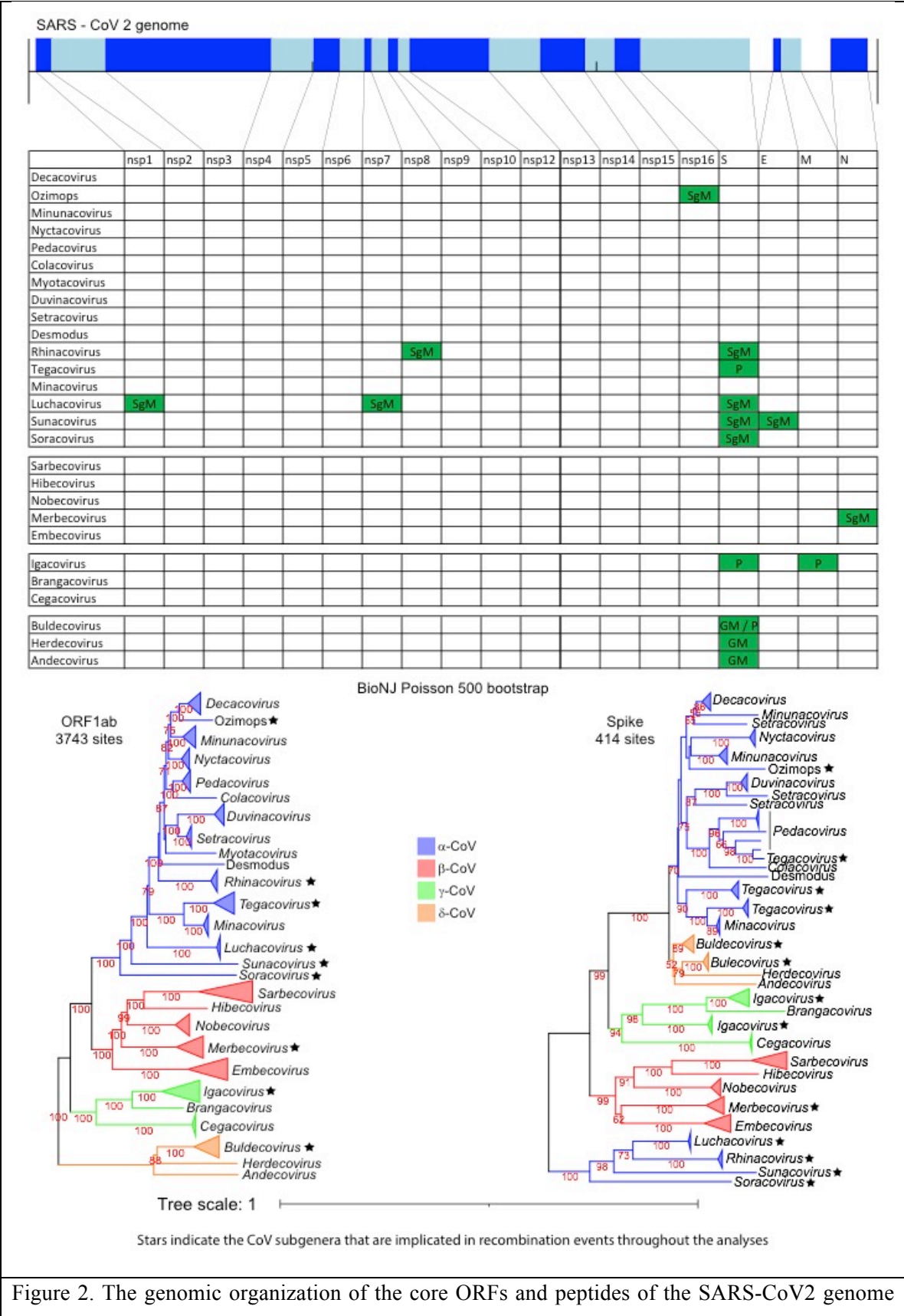


Figure 2. The genomic organization of the core ORFs and peptides of the SARS-CoV2 genome

are displayed on the top of the figure. The table/matrix below it shows which genomic regions of the various subgenera are involved in intertypic recombination events. “GM” represents events that occurred at the common ancestor of the genus. “SgM” represents events that occurred at the common ancestor of the subgenus. “P” represents more recent events that occurred for one or few members of the subgenus and have resulted in a polyphyletic tree pattern (for that region and subgenus). All incongruence events in the matrix are supported by the three phylogenetic tree methods (NJ, PhyML, Bayesian) and are also statistically significant, based on the approximately unbiased test of CONSEL. Two phylogenetic trees (of ORF1ab and Spike) for all four genera are also included below the matrix, to visualize the recombination events of the Spike region. In these trees, we use stars to denote sub-genera that have been involved in intertypic homologous recombination events, in any genomic region (not only the Spike).

483

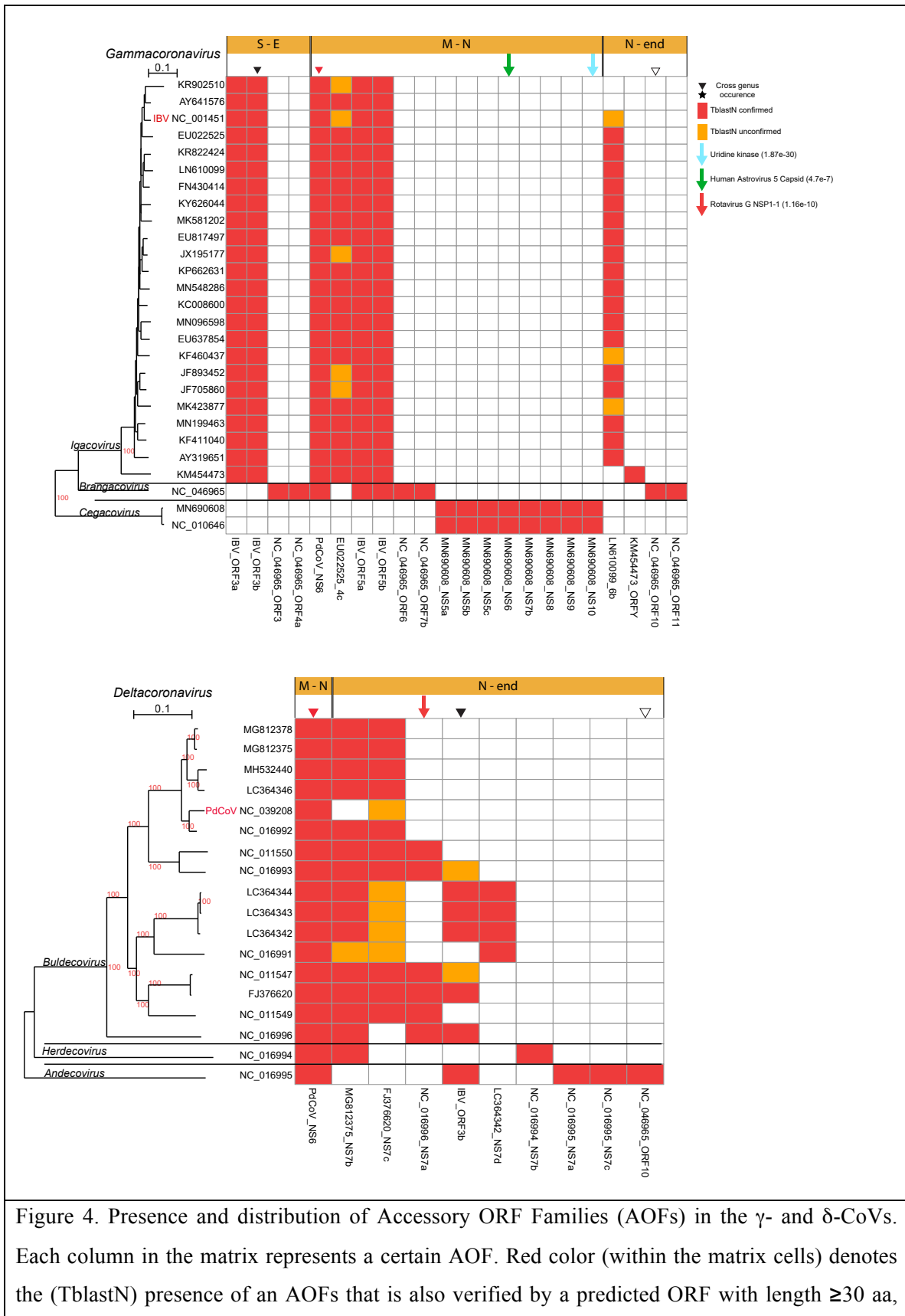
484

485



Figure 3. Presence and distribution of Accessory ORF Families (AOFs) in the  $\alpha$ - and  $\beta$ -CoVs. Each column in the matrix represents a certain AOF. Red color (within the matrix cells) denotes the (TblastN) presence of an AOF that is also verified by a predicted ORF with length  $\geq 30$  aa, whereas if the length of the predicted ORF is  $< 30$  aa, then it is denoted with orange color. Stars

denote AOFs that are present in both  $\alpha$ - and  $\beta$ -CoV members, whereas diamonds denote an AOF that resulted from duplication of a core ORF. Downward arrows denote AOFs that have homologs in non-CoV genomes, together with their best PSI-Blast hit e-value. Horizontal orange bars (above the matrices) denote the genomic region where the AOF is located, i.e. S-E denotes the region between the Spike and Envelope ORFs.



whereas if the length of the predicted ORF is  $<30$  aa, then it is denoted with orange color. Inverted triangles denote AOFs that are present in both  $\gamma$ - and  $\delta$ -CoV members. Downward arrows denote AOFs that have homologs in non-CoV genomes, together with their best PSI-Blast hit e-value. Horizontal orange bars (above the matrices) denote the genomic region where the AOF is located, i.e. M-N denotes the region between the Membrane and Nucleocapsid ORFs.

487

488 **Availability of Data:** All necessary data are incorporated into the article and its online  
489 supplementary material. Any further data are available on request.

490 **Contributions:** M.N and G.D.A. analyzed the data; M.N, P.M., Y.V.d.P., S.G.O., G.D.A  
491 designed the analyses, wrote and edited the manuscript; G.D.A. supervised M.N.

492 **Acknowledgements:** M.N. would like to thank the Bodossakis foundation (studentship: BDA-  
493 394) and the University of Thessaly (studentship: DEKA-UTH-259) for financial support. We  
494 thank Stephane Rombauts for useful discussions concerning bacterial genome assembly artefacts.

495 **Competing interests:** The authors declare no competing interests.

496

#### 497 **References**

498 Banerjee A, Doxey AC, Tremblay BJ-M, Mansfield MJ, Subudhi S, Hirota JA, Miller MS,  
499 McArthur AG, Mubareka S, Mossman K. 2020. Predicting the recombination  
500 potential of severe acute respiratory syndrome coronavirus 2 and Middle  
501 East respiratory syndrome coronavirus. *J Gen Virol*.

502 Bankevich A, Nurk S, Antipov D, Gurevich AA, Dvorkin M, Kulikov AS, Lesin VM,  
503 Nikolenko SI, Pham S, Prjibelski AD, et al. 2012. SPAdes: a new genome  
504 assembly algorithm and its applications to single-cell sequencing. *J Comput  
505 Biol* 19:455–477.

506 Bedford J, Farrar J, Ihekweazu C, Kang G, Koopmans M, Nkengasong J. 2019. A new  
507 twenty-first century science for effective epidemic response. *Nature*  
508 575:130–136.

509 Benson DA, Cavanaugh M, Clark K, Karsch-Mizrachi I, Lipman DJ, Ostell J, Sayers EW.  
510 2013. GenBank. *Nucleic Acids Res.* 41:D36-42.

511 Bermingham A, Chand MA, Brown CS, Aarons E, Tong C, Langrish C, Hoschler K,  
512 Brown K, Galiano M, Myers R, et al. 2012. Severe respiratory illness caused by  
513 a novel coronavirus, in a patient transferred to the United Kingdom from the  
514 Middle East, September 2012. *Euro Surveill.* 17:20290.

- 515 Beyer RM, Manica A, Mora C. 2021. Shifts in global bat diversity suggest a possible  
516 role of climate change in the emergence of SARS-CoV-1 and SARS-CoV-2. *Sci*  
517 *Total Environ*:145413.
- 518 Bobay L-M, O'Donnell AC, Ochman H. 2020. Recombination events are concentrated  
519 in the spike protein region of Betacoronaviruses. *PLoS Genet* 16:e1009272.
- 520 Boley PA, Alhamo MA, Lossie G, Yadav KK, Vasquez-Lee M, Saif LJ, Kenney SP. 2020.  
521 Porcine Deltacoronavirus Infection and Transmission in Poultry, United  
522 States1. *Emerging Infectious Diseases* 26:255–265.
- 523 Boni MF, Lemey P, Jiang X, Lam TT-Y, Perry BW, Castoe TA, Rambaut A, Robertson  
524 DL. 2020. Evolutionary origins of the SARS-CoV-2 sarbecovirus lineage  
525 responsible for the COVID-19 pandemic. *Nat Microbiol*.
- 526 Boniotti MB, Papetti A, Lavazza A, Alborali G, Sozzi E, Chiapponi C, Faccini S,  
527 Bonilauri P, Cordioli P, Marthaler D. 2016. Porcine Epidemic Diarrhea Virus  
528 and Discovery of a Recombinant Swine Enteric Coronavirus, Italy. *Emerg*  
529 *Infect Dis* 22:83–87.
- 530 Burns CC, Shaw J, Jorba J, Bukbuk D, Adu F, Gumede N, Pate MA, Abanida EA,  
531 Gasasira A, Iber J, et al. 2013. Multiple independent emergences of type 2  
532 vaccine-derived polioviruses during a large outbreak in northern Nigeria. *J*  
533 *Viol.* 87:4907–4922.
- 534 Caprari S, Metzler S, Lengauer T, Kalinina OV. 2015. Sequence and Structure  
535 Analysis of Distantly-Related Viruses Reveals Extensive Gene Transfer  
536 between Viruses and Hosts and among Viruses. *Viruses* 7:5388–5409.
- 537 Casais R, Dove B, Cavanagh D, Britton P. 2003. Recombinant avian infectious  
538 bronchitis virus expressing a heterologous spike gene demonstrates that the  
539 spike protein is a determinant of cell tropism. *J Virol* 77:9084–9089.
- 540 Castresana J. 2000. Selection of conserved blocks from multiple alignments for their  
541 use in phylogenetic analysis. *Mol Biol Evol* 17:540–552.
- 542 Chen Y, Liu Q, Guo D. 2020. Emerging coronaviruses: Genome structure, replication,  
543 and pathogenesis. *J. Med. Virol.* 92:418–423.
- 544 Chevenet F, Brun C, Bañuls A-L, Jacq B, Christen R. 2006. TreeDyn: towards dynamic  
545 graphics and annotations for analyses of trees. *BMC Bioinformatics* 7:439.
- 546 Coronaviridae Study Group of the International Committee on Taxonomy of Viruses.  
547 2020. The species Severe acute respiratory syndrome-related coronavirus:  
548 classifying 2019-nCoV and naming it SARS-CoV-2. *Nat Microbiol* 5:536–544.

- 549 Cui J, Li F, Shi Z-L. 2019. Origin and evolution of pathogenic coronaviruses. *Nat. Rev.*  
550 *Microbiol.* 17:181–192.
- 551 Darriba D, Taboada GL, Doallo R, Posada D. 2011. ProtTest 3: fast selection of best-fit  
552 models of protein evolution. *Bioinformatics* 27:1164–1165.
- 553 Decaro N, Mari V, Campolo M, Lorusso A, Camero M, Elia G, Martella V, Cordioli P,  
554 Enjuanes L, Buonavoglia C. 2009. Recombinant canine coronaviruses related  
555 to transmissible gastroenteritis virus of Swine are circulating in dogs. *J Virol*  
556 83:1532–1537.
- 557 Drummond AJ, Suchard MA, Xie D, Rambaut A. 2012. Bayesian Phylogenetics with  
558 BEAUti and the BEAST 1.7. *Molecular Biology and Evolution* 29:1969–1973.
- 559 Dudas G, Rambaut A. 2016. MERS-CoV recombination: implications about the  
560 reservoir and potential for adaptation. *Virus Evolution* 2:vev023.
- 561 Edgar RC. 2004. MUSCLE: multiple sequence alignment with high accuracy and high  
562 throughput. *Nucleic Acids Res.* 32:1792–1797.
- 563 Edgar RC. 2010. Search and clustering orders of magnitude faster than BLAST.  
564 *Bioinformatics* 26:2460–2461.
- 565 Elhaik E, Sabath N, Graur D. 2006. The “inverse relationship between evolutionary  
566 rate and age of mammalian genes” is an artifact of increased genetic distance  
567 with rate of evolution and time of divergence. *Mol Biol Evol* 23:1–3.
- 568 Enright AJ, Van Dongen S, Ouzounis CA. 2002. An efficient algorithm for large-scale  
569 detection of protein families. *Nucleic Acids Res* 30:1575–1584.
- 570 Fan Y, Zhao K, Shi Z-L, Zhou P. 2019. Bat Coronaviruses in China. *Viruses* 11.
- 571 Forni D, Cagliani R, Clerici M, Sironi M. 2017. Molecular Evolution of Human  
572 Coronavirus Genomes. *Trends Microbiol* 25:35–48.
- 573 Gilbert C, Cordaux R. 2017. Viruses as vectors of horizontal transfer of genetic  
574 material in eukaryotes. *Curr Opin Virol* 25:16–22.
- 575 Goldstein SA, Brown J, Pedersen BS, Quinlan AR, Elde NC. 2021. Extensive  
576 recombination-driven coronavirus diversification expands the pool of  
577 potential pandemic pathogens. *bioRxiv*.
- 578 Goluch T, Bogdanowicz D, Giaro K. 2020. Visual TreeCmp: Comprehensive  
579 Comparison of Phylogenetic Trees on the Web. Price S, editor. *Methods in*  
580 *Ecology and Evolution* 11:494–499.
- 581 Gorbalenya AE, Enjuanes L, Ziebuhr J, Snijder EJ. 2006. Nidovirales: Evolving the  
582 largest RNA virus genome. *Virus Research* 117:17–37.



- 583 Gouy M, Guindon S, Gascuel O. 2010. SeaView version 4: A multiplatform graphical  
584 user interface for sequence alignment and phylogenetic tree building. *Mol.*  
585 *Biol. Evol.* 27:221–224.
- 586 Graham RL, Baric RS. 2010. Recombination, reservoirs, and the modular spike:  
587 mechanisms of coronavirus cross-species transmission. *Journal of Virology*  
588 84:3134–3146.
- 589 Graham RL, Deming DJ, Deming ME, Yount BL, Baric RS. 2018. Evaluation of a  
590 recombination-resistant coronavirus as a broadly applicable, rapidly  
591 implementable vaccine platform. *Commun Biol* 1:179.
- 592 Guillot S, Caro V, Cuervo N, Korotkova E, Combiescu M, Persu A, Aubert-Combiescu  
593 A, Delpeyroux F, Crainic R. 2000. Natural genetic exchanges between vaccine  
594 and wild poliovirus strains in humans. *J. Virol.* 74:8434–8443.
- 595 Guindon S, Gascuel O. 2003. A simple, fast, and accurate algorithm to estimate large  
596 phylogenies by maximum likelihood. *Syst. Biol.* 52:696–704.
- 597 Hartenian E, Nandakumar D, Lari A, Ly M, Tucker JM, Glaunsinger BA. 2020. The  
598 molecular virology of coronaviruses. *J Biol Chem* 295:12910–12934.
- 599 Henritzi D, Petric PP, Lewis NS, Graaf A, Pessia A, Starick E, Breithaupt A, Strebelow  
600 G, Luttermann C, Parker LMK, et al. 2020. Surveillance of European Domestic  
601 Pig Populations Identifies an Emerging Reservoir of Potentially Zoonotic  
602 Swine Influenza A Viruses. *Cell Host Microbe* 28:614-627.e6.
- 603 Herrewegh AA, Smeenk I, Horzinek MC, Rottier PJ, de Groot RJ. 1998. Feline  
604 coronavirus type II strains 79-1683 and 79-1146 originate from a double  
605 recombination between feline coronavirus type I and canine coronavirus. *J*  
606 *Virology* 72:4508–4514.
- 607 Hu Z-M, Yang Y-L, Xu L-D, Wang B, Qin P, Huang Y-W. 2019. Porcine Torovirus  
608 (PToV)—A Brief Review of Etiology, Diagnostic Assays and Current  
609 Epidemiology. *Frontiers in Veterinary Science* [Internet] 6. Available from:  
610 <https://www.frontiersin.org/article/10.3389/fvets.2019.00120/full>
- 611 Huang C, Liu WJ, Xu W, Jin T, Zhao Y, Song J, Shi Y, Ji W, Jia H, Zhou Y, et al. 2016. A  
612 Bat-Derived Putative Cross-Family Recombinant Coronavirus with a  
613 Reovirus Gene. *PLoS Pathog* 12:e1005883.
- 614 Huson DH, Scornavacca C. 2012. Dendroscope 3: an interactive tool for rooted  
615 phylogenetic trees and networks. *Syst Biol* 61:1061–1067.
- 616 ICTV Coronaviridae study group. International Committee on Taxonomy of Viruses  
617 (ICTV). Available from: <https://talk.ictvonline.org/ictv->

618 reports/ictv\_9th\_report/positive-sense-rna-viruses-  
619 2011/w/posrna\_viruses/223/coronaviridae-figures

620 Keck JG, Matsushima GK, Makino S, Fleming JO, Vannier DM, Stohlman SA, Lai MM.  
621 1988. In vivo RNA-RNA recombination of coronavirus in mouse brain. *J Virol*  
622 62:1810–1813.

623 Kemp SA, Collier DA, Datir RP, Ferreira IATM, Gayed S, Jahun A, Hosmillo M, Rees-  
624 Spear C, Mlcochova P, Lumb IU, et al. 2021. SARS-CoV-2 evolution during  
625 treatment of chronic infection. *Nature*.

626 Kottier SA, Cavanagh D, Britton P. 1995. Experimental evidence of recombination in  
627 coronavirus infectious bronchitis virus. *Virology* 213:569–580.

628 Kumar S, Stecher G, Li M, Knyaz C, Tamura K. 2018. MEGA X: Molecular Evolutionary  
629 Genetics Analysis across Computing Platforms. *Mol Biol Evol* 35:1547–1549.

630 Kuo L, Godeke GJ, Raamsman MJ, Masters PS, Rottier PJ. 2000. Retargeting of  
631 coronavirus by substitution of the spike glycoprotein ectodomain: crossing  
632 the host cell species barrier. *J Virol* 74:1393–1406.

633 Lam TT-Y, Jia N, Zhang Y-W, Shum MH-H, Jiang J-F, Zhu H-C, Tong Y-G, Shi Y-X, Ni X-  
634 B, Liao Y-S, et al. 2020. Identifying SARS-CoV-2-related coronaviruses in  
635 Malayan pangolins. *Nature* 583:282–285.

636 Lang Y, Li W, Li Z, Koerhuis D, van den Burg ACS, Rozemuller E, Bosch B-J, van  
637 Kuppeveld FJM, Boons G-J, Huizinga EG, et al. 2020. Coronavirus  
638 hemagglutinin-esterase and spike proteins coevolve for functional balance  
639 and optimal virion avidity. *Proc Natl Acad Sci U S A* 117:25759–25770.

640 Latinne A, Hu B, Olival KJ, Zhu G, Zhang L, Li H, Chmura AA, Field HE, Zambrana-  
641 Torrelío C, Epstein JH, et al. 2020. Origin and cross-species transmission of  
642 bat coronaviruses in China. *Nat Commun* 11:4235.

643 Lau SKP, Wong EYM, Tsang C-C, Ahmed SS, Au-Yeung RKH, Yuen K-Y, Wernery U,  
644 Woo PCY. 2018. Discovery and Sequence Analysis of Four Deltacoronaviruses  
645 from Birds in the Middle East Reveal Interspecies Jumping with  
646 Recombination as a Potential Mechanism for Avian-to-Avian and Avian-to-  
647 Mammalian Transmission. *J Virol* 92.

648 Lauber C, Goeman JJ, Parquet M del C, Thi Nga P, Snijder EJ, Morita K, Gorbalenya AE.  
649 2013. The Footprint of Genome Architecture in the Largest Genome  
650 Expansion in RNA Viruses. Stern A, editor. *PLoS Pathogens* 9:e1003500.

651 Lauber C, Gorbalenya AE. 2012. Partitioning the genetic diversity of a virus family:  
652 approach and evaluation through a case study of picornaviruses. *J. Virol.*  
653 86:3890–3904.



- 655 Lauber C, Ziebuhr J, Junglen S, Drosten C, Zirkel F, Nga PT, Morita K, Snijder EJ,  
656 Gorbalenya AE. 2012. Mesoniviridae: a proposed new family in the order  
657 Nidovirales formed by a single species of mosquito-borne viruses. *Arch. Virol.*  
658 157:1623–1628.
- 659 Letunic I, Bork P. 2019. Interactive Tree Of Life (iTOL) v4: recent updates and new  
660 developments. *Nucleic Acids Res* 47:W256–W259.
- 661 Li W, Hulswit RJG, Kenney SP, Widjaja I, Jung K, Alhamo MA, van Dieren B, van  
662 Kuppeveld FJM, Saif LJ, Bosch B-J. 2018. Broad receptor engagement of an  
663 emerging global coronavirus may potentiate its diverse cross-species  
664 transmissibility. *Proceedings of the National Academy of Sciences of the United*  
665 *States of America* 115:E5135–E5143.
- 666 Li W, Wong S-K, Li F, Kuhn JH, Huang I-C, Choe H, Farzan M. 2006. Animal origins of  
667 the severe acute respiratory syndrome coronavirus: insight from ACE2-S-  
668 protein interactions. *J Virol* 80:4211–4219.
- 669 Liu DX, Fung TS, Chong KK-L, Shukla A, Hilgenfeld R. 2014. Accessory proteins of  
670 SARS-CoV and other coronaviruses. *Antiviral Research* 109:97–109.
- 671 Lo C-Y, Tsai T-L, Lin C-N, Lin C-H, Wu H-Y. 2019. Interaction of coronavirus  
672 nucleocapsid protein with the 5'- and 3'-ends of the coronavirus genome is  
673 involved in genome circularization and negative-strand RNA synthesis. *FEBS*  
674 *J.* 286:3222–3239.
- 675 Martin DP, Lemey P, Posada D. 2011. Analysing recombination in nucleotide  
676 sequences. *Mol Ecol Resour* 11:943–955.
- 677 Martin DP, Murrell B, Golden M, Khoosal A, Muhire B. 2015. RDP4: Detection and  
678 analysis of recombination patterns in virus genomes. *Virus Evolution*  
679 1:vev003–vev003.
- 680 Masters PS. 2019. Coronavirus genomic RNA packaging. *Virology* 537:198–207.
- 681 Mazumder R, Iyer LM, Vasudevan S, Aravind L. 2002. Detection of novel members,  
682 structure-function analysis and evolutionary classification of the 2H  
683 phosphoesterase superfamily. *Nucleic Acids Res* 30:5229–5243.
- 684 McLysaght A, Hurst LD. 2016. Open questions in the study of de novo genes: what,  
685 how and why. *Nat Rev Genet* 17:567–578.
- 686 Meekins DA, Morozov I, Trujillo JD, Gaudreault NN, Bold D, Carossino M, Artiaga BL,  
687 Indran SV, Kwon T, Balaraman V, et al. 2020. Susceptibility of swine cells and  
688 domestic pigs to SARS-CoV-2. *Emerg Microbes Infect* 9:2278–2288.

689 Menachery VD, Yount BL, Debbink K, Agnihothram S, Gralinski LE, Plante JA, Graham  
690 RL, Scobey T, Ge X-Y, Donaldson EF, et al. 2015. A SARS-like cluster of  
691 circulating bat coronaviruses shows potential for human emergence. *Nature*  
692 *Medicine* 21:1508–1513.

693 Menachery VD, Yount BL, Sims AC, Debbink K, Agnihothram SS, Gralinski LE,  
694 Graham RL, Scobey T, Plante JA, Royal SR, et al. 2016. SARS-like WIV1-CoV  
695 poised for human emergence. *Proceedings of the National Academy of*  
696 *Sciences of the United States of America* 113:3048–3053.

697 Mihindukulasuriya KA, Wu G, St Leger J, Nordhausen RW, Wang D. 2008.  
698 Identification of a novel coronavirus from a beluga whale by using a panviral  
699 microarray. *J Virol* 82:5084–5088.

700 de Moraes HA, Dos Santos AP, do Nascimento NC, Kmetiuk LB, Barbosa DS, Brandão  
701 PE, Guimarães AMS, Pettan-Brewer C, Biondo AW. 2020. Natural Infection by  
702 SARS-CoV-2 in Companion Animals: A Review of Case Reports and Current  
703 Evidence of Their Role in the Epidemiology of COVID-19. *Front Vet Sci*  
704 7:591216.

705 Moyers BA, Zhang J. 2016. Evaluating Phylostratigraphic Evidence for Widespread  
706 De Novo Gene Birth in Genome Evolution. *Mol Biol Evol* 33:1245–1256.

707 Nakamura T, Yamada KD, Tomii K, Katoh K. 2018. Parallelization of MAFFT for  
708 large-scale multiple sequence alignments. *Bioinformatics* 34:2490–2492.

709 Neches RY, Kyrpides NC, Ouzounis CA. 2021. Atypical Divergence of SARS-CoV-2  
710 Orf8 from Orf7a within the Coronavirus Lineage Suggests Potential Stealthy  
711 Viral Strategies in Immune Evasion. *mBio* 12.

712 Neches RY, McGee MD, Kyrpides NC. 2020. Recombination should not be an  
713 afterthought. *Nat Rev Microbiol* 18:606.

714 Nikolaidis M, Mimouli K, Kyriakopoulou Z, Tsimpidis M, Tsakogiannis D,  
715 Markoulatos P, Amoutzias GD. 2019. Large-scale genomic analysis reveals  
716 recurrent patterns of intertypic recombination in human enteroviruses.  
717 *Virology* 526:72–80.

718 Olival KJ, Cryan PM, Amman BR, Baric RS, Blehert DS, Brook CE, Calisher CH, Castle  
719 KT, Coleman JTH, Daszak P, et al. 2020. Possibility for reverse zoonotic  
720 transmission of SARS-CoV-2 to free-ranging wildlife: A case study of bats.  
721 *PLoS Pathog.* 16:e1008758.

722 Ouzounis CA. 2020. A recent origin of Orf3a from M protein across the coronavirus  
723 lineage arising by sharp divergence. *Comput Struct Biotechnol J* 18:4093–  
724 4102.

- 725 Paraskevis D, Kostaki EG, Magiorkinis G, Panayiotakopoulos G, Sourvinos G,  
726 Tsiodras S. 2020. Full-genome evolutionary analysis of the novel corona  
727 virus (2019-nCoV) rejects the hypothesis of emergence as a result of a recent  
728 recombination event. *Infect Genet Evol* 79:104212.
- 729 Pickering BS, Smith G, Pinette MM, Embury-Hyatt C, Moffat E, Marszal P, Lewis CE.  
730 2021. Susceptibility of Domestic Swine to Experimental Infection with Severe  
731 Acute Respiratory Syndrome Coronavirus 2. *Emerg Infect Dis* 27:104–112.
- 732 Pliaka V, Kyriakopoulou Z, Markoulatos P. 2012. Risks associated with the use of  
733 live-attenuated vaccine poliovirus strains and the strategies for control and  
734 eradication of paralytic poliomyelitis. *Expert Rev Vaccines* 11:609–628.
- 735 Pond SLK, Frost SDW, Muse SV. 2005. HyPhy: hypothesis testing using phylogenies.  
736 *Bioinformatics* 21:676–679.
- 737 Posada D, Crandall KA, Holmes EC. 2002. Recombination in Evolutionary Genomics.  
738 *Annual Review of Genetics* 36:75–97.
- 739 Racaniello VR. 2006. One hundred years of poliovirus pathogenesis. *Virology* 344:9–  
740 16.
- 741 Reusken CB, Haagmans BL, Müller MA, Gutierrez C, Godeke G-J, Meyer B, Muth D, Raj  
742 VS, Vries LS-D, Corman VM, et al. 2013. Middle East respiratory syndrome  
743 coronavirus neutralising serum antibodies in dromedary camels: a  
744 comparative serological study. *The Lancet Infectious Diseases* 13:859–866.
- 745 Robinson DF, Foulds LR. 1981. Comparison of phylogenetic trees. *Mathematical*  
746 *Biosciences* 53:131–147.
- 747 Rota PA, Oberste MS, Monroe SS, Nix WA, Campagnoli R, Icenogle JP, Peñaranda S,  
748 Bankamp B, Maher K, Chen M-H, et al. 2003. Characterization of a novel  
749 coronavirus associated with severe acute respiratory syndrome. *Science*  
750 300:1394–1399.
- 751 Rottier PJM, Nakamura K, Schellen P, Volders H, Haijema BJ. 2005. Acquisition of  
752 macrophage tropism during the pathogenesis of feline infectious peritonitis  
753 is determined by mutations in the feline coronavirus spike protein. *J Virol*  
754 79:14122–14130.
- 755 Saeng-Chuto K, Jermsutjarit P, Stott CJ, Vui DT, Tantituvanont A, Nilubol D. 2020.  
756 Retrospective study, full-length genome characterization and evaluation of  
757 viral infectivity and pathogenicity of chimeric porcine deltacoronavirus  
758 detected in Vietnam. *Transbound Emerg Dis* 67:183–198.
- 759 Sánchez CM, Izeta A, Sánchez-Morgado JM, Alonso S, Sola I, Balasch M, Plana-Durán J,  
760 Enjuanes L. 1999. Targeted recombination demonstrates that the spike gene

- 761 of transmissible gastroenteritis coronavirus is a determinant of its enteric  
762 tropism and virulence. *J Virol* 73:7607–7618.
- 763 Sawicki SG, Sawicki DL, Siddell SG. 2007. A contemporary view of coronavirus  
764 transcription. *J Virol* 81:20–29.
- 765 Schelle B, Karl N, Ludewig B, Siddell SG, Thiel V. 2005. Selective replication of  
766 coronavirus genomes that express nucleocapsid protein. *J. Virol.* 79:6620–  
767 6630.
- 768 Schmitz JF, Bornberg-Bauer E. 2017. Fact or fiction: updates on how protein-coding  
769 genes might emerge de novo from previously non-coding DNA.  
770 *F1000Research* 6:57.
- 771 Shang J, Zheng Y, Yang Y, Liu C, Geng Q, Tai W, Du L, Zhou Y, Zhang W, Li F. 2018.  
772 Cryo-Electron Microscopy Structure of Porcine Deltacoronavirus Spike  
773 Protein in the Prefusion State. *J Virol* 92.
- 774 Shang P, Misra S, Hause B, Fang Y. 2017. A Naturally Occurring Recombinant  
775 Enterovirus Expresses a Torovirus Deubiquitinase. Perlman S, editor. *Journal*  
776 *of Virology* [Internet] 91. Available from:  
777 <https://jvi.asm.org/lookup/doi/10.1128/JVI.00450-17>
- 778 Shi J, Wen Z, Zhong G, Yang H, Wang C, Huang B, Liu R, He X, Shuai L, Sun Z, et al.  
779 2020. Susceptibility of ferrets, cats, dogs, and other domesticated animals to  
780 SARS-coronavirus 2. *Science* 368:1016–1020.
- 781 Shimodaira H, Hasegawa M. 2001. CONSEL: for assessing the confidence of  
782 phylogenetic tree selection. *Bioinformatics* 17:1246–1247.
- 783 Simon-Loriere E, Holmes EC. 2011. Why do RNA viruses recombine? *Nat. Rev.*  
784 *Microbiol.* 9:617–626.
- 785 Sit THC, Brackman CJ, Ip SM, Tam KWS, Law PYT, To EMW, Yu VYT, Sims LD, Tsang  
786 DNC, Chu DKW, et al. 2020. Infection of dogs with SARS-CoV-2. *Nature*  
787 586:776–778.
- 788 Snijder EJ, den Boon JA, Horzinek MC, Spaan WJ. 1991. Comparison of the genome  
789 organization of toro- and coronaviruses: evidence for two nonhomologous  
790 RNA recombination events during Berne virus evolution. *Virology* 180:448–  
791 452.
- 792 Sola I, Almazán F, Zúñiga S, Enjuanes L. 2015. Continuous and Discontinuous RNA  
793 Synthesis in Coronaviruses. *Annu Rev Virol* 2:265–288.

- 794 Sola I, Mateos-Gomez PA, Almazan F, Zuñiga S, Enjuanes L. 2011. RNA-RNA and  
795 RNA-protein interactions in coronavirus replication and transcription. *RNA*  
796 *Biol* 8:237–248.
- 797 Song H-D, Tu C-C, Zhang G-W, Wang S-Y, Zheng K, Lei L-C, Chen Q-X, Gao Y-W, Zhou  
798 H-Q, Xiang H, et al. 2005. Cross-host evolution of severe acute respiratory  
799 syndrome coronavirus in palm civet and human. *Proc. Natl. Acad. Sci. U.S.A.*  
800 102:2430–2435.
- 801 Stöver BC, Müller KF. 2010. TreeGraph 2: combining and visualizing evidence from  
802 different phylogenetic analyses. *BMC Bioinformatics* 11:7.
- 803 Su S, Wong G, Shi W, Liu J, Lai ACK, Zhou J, Liu W, Bi Y, Gao GF. 2016. Epidemiology,  
804 Genetic Recombination, and Pathogenesis of Coronaviruses. *Trends Microbiol.*  
805 24:490–502.
- 806 Suchard MA, Lemey P, Baele G, Ayres DL, Drummond AJ, Rambaut A. 2018. Bayesian  
807 phylogenetic and phylodynamic data integration using BEAST 1.10. *Virus*  
808 *Evolution* [Internet] 4. Available from:  
809 <https://academic.oup.com/ve/article/doi/10.1093/ve/vey016/5035211>
- 810 Sun Honglei, Xiao Y, Liu Jiyu, Wang D, Li F, Wang C, Li C, Zhu J, Song J, Sun Haoran, et  
811 al. 2020. Prevalent Eurasian avian-like H1N1 swine influenza virus with 2009  
812 pandemic viral genes facilitating human infection. *Proc Natl Acad Sci U S A*  
813 117:17204–17210.
- 814 Sungsuwan S, Jongkaewwattana A, Jaru-Ampornpan P. 2020. Nucleocapsid proteins  
815 from other swine enteric coronaviruses differentially modulate PEDV  
816 replication. *Virology* 540:45–56.
- 817 Terada Y, Matsui N, Noguchi K, Kuwata R, Shimoda H, Soma T, Mochizuki M, Maeda  
818 K. 2014. Emergence of pathogenic coronaviruses in cats by homologous  
819 recombination between feline and canine coronaviruses. *PLoS One*  
820 9:e106534.
- 821 Tian P-F, Jin Y-L, Xing G, Qv L-L, Huang Y-W, Zhou J-Y. 2014. Evidence of  
822 recombinant strains of porcine epidemic diarrhea virus, United States, 2013.  
823 *Emerg Infect Dis* 20:1735–1738.
- 824 Tsoleridis T, Chappell JG, Onianwa O, Marston DA, Fooks AR, Monchatre-Leroy E,  
825 Umhang G, Müller MA, Drexler JF, Drosten C, et al. 2019. Shared Common  
826 Ancestry of Rodent Alphacoronaviruses Sampled Globally. *Viruses* 11.
- 827 Volz E, Hill V, McCrone JT, Price A, Jorgensen D, O'Toole Á, Southgate J, Johnson R,  
828 Jackson B, Nascimento FF, et al. 2021. Evaluating the Effects of SARS-CoV-2  
829 Spike Mutation D614G on Transmissibility and Pathogenicity. *Cell* 184:64-  
830 75.e11.



- 831 Wang W, Lin X-D, Zhang H-L, Wang M-R, Guan X-Q, Holmes EC, Zhang Y-Z. 2020.  
832 Extensive Genetic Diversity And Host Range Of Rodent-Borne Coronaviruses.  
833 *Virus Evolution* [Internet]. Available from:  
834 [https://academic.oup.com/ve/advance-](https://academic.oup.com/ve/advance-article/doi/10.1093/ve/veaa078/5934349)  
835 [article/doi/10.1093/ve/veaa078/5934349](https://academic.oup.com/ve/advance-article/doi/10.1093/ve/veaa078/5934349)
- 836 Weiss SR, Navas-Martin S. 2005. Coronavirus pathogenesis and the emerging  
837 pathogen severe acute respiratory syndrome coronavirus. *Microbiol. Mol.*  
838 *Biol. Rev.* 69:635–664.
- 839 Wheeler DL, Sariol A, Meyerholz DK, Perlman S. 2018. Microglia are required for  
840 protection against lethal coronavirus encephalitis in mice. *J Clin Invest*  
841 128:931–943.
- 842 Wille M, Holmes EC. 2020. Wild birds as reservoirs for diverse and abundant  
843 gamma- and deltacoronaviruses. *FEMS microbiology reviews* 44:631–644.
- 844 Wong ACP, Li X, Lau SKP, Woo PCY. 2019. Global Epidemiology of Bat Coronaviruses.  
845 *Viruses* 11.
- 846 Woo PCY, Lau SKP, Huang Y, Yuen K-Y. 2009. Coronavirus diversity, phylogeny and  
847 interspecies jumping. *Exp. Biol. Med. (Maywood)* 234:1117–1127.
- 848 Woo PCY, Lau SKP, Lam CSF, Lau CCY, Tsang AKL, Lau JHN, Bai R, Teng JLL, Tsang  
849 CCC, Wang M, et al. 2012. Discovery of seven novel Mammalian and avian  
850 coronaviruses in the genus deltacoronavirus supports bat coronaviruses as  
851 the gene source of alphacoronavirus and betacoronavirus and avian  
852 coronaviruses as the gene source of gammacoronavirus and  
853 deltacoronavirus. *J. Virol.* 86:3995–4008.
- 854 Woo PCY, Lau SKP, Lam CSF, Tsang AKL, Hui S-W, Fan RYY, Martelli P, Yuen K-Y.  
855 2014. Discovery of a novel bottlenose dolphin coronavirus reveals a distinct  
856 species of marine mammal coronavirus in Gammacoronavirus. *J Virol*  
857 88:1318–1331.
- 858 Woo PCY, Wang M, Lau SKP, Xu H, Poon RWS, Guo R, Wong BHL, Gao K, Tsoi H-W,  
859 Huang Y, et al. 2007. Comparative analysis of twelve genomes of three novel  
860 group 2c and group 2d coronaviruses reveals unique group and subgroup  
861 features. *J. Virol.* 81:1574–1585.
- 862 Worobey M, Pekar J, Larsen BB, Nelson MI, Hill V, Joy JB, Rambaut A, Suchard MA,  
863 Wertheim JO, Lemey P. 2020. The emergence of SARS-CoV-2 in Europe and  
864 North America. *Science* 370:564–570.
- 865 Wu F, Zhao S, Yu B, Chen Y-M, Wang W, Song Z-G, Hu Y, Tao Z-W, Tian J-H, Pei Y-Y, et  
866 al. 2020. A new coronavirus associated with human respiratory disease in  
867 China. *Nature* 579:265–269.

- 868 Yang Y, Yan W, Hall AB, Jiang X. 2021. Characterizing Transcriptional Regulatory  
869 Sequences in Coronaviruses and Their Role in Recombination. *Mol Biol Evol*  
870 38:1241–1248.
- 871 Yount B, Roberts RS, Lindesmith L, Baric RS. 2006. Rewiring the severe acute  
872 respiratory syndrome coronavirus (SARS-CoV) transcription circuit:  
873 engineering a recombination-resistant genome. *Proc Natl Acad Sci U S A*  
874 103:12546–12551.
- 875 Zeng Q, Langereis MA, van Vliet ALW, Huizinga EG, de Groot RJ. 2008. Structure of  
876 coronavirus hemagglutinin-esterase offers insight into corona and influenza  
877 virus evolution. *Proc Natl Acad Sci U S A* 105:9065–9069.
- 878 Ziv O, Price J, Shalamova L, Kamenova T, Goodfellow I, Weber F, Miska EA. 2020. The  
879 Short- and Long-Range RNA-RNA Interactome of SARS-CoV-2. *Mol Cell*  
880 80:1067-1077.e5.
- 881 Züst R, Miller TB, Goebel SJ, Thiel V, Masters PS. 2008. Genetic interactions between  
882 an essential 3' cis-acting RNA pseudoknot, replicase gene products, and the  
883 extreme 3' end of the mouse coronavirus genome. *J. Virol.* 82:1214–1228.
- 884